

8. IJRER

By Siti Jamilatun

Non-catalytic and Catalytic Pyrolysis of *Spirulina platensis* residue (SPR) in Fixed-Bed Reactors: Characteristic and Kinetic Study with Primary and Secondary Tar Cracking Models

Siti Jamilatun^{*‡}, Endah Sulistiawati^{*}, Shinta Amelia^{*}, Arief Budiman^{**}

^{*} Department of Chemical Engineering, Faculty of Industrial Technology, Universitas Ahmad Dahlan, Jl. Ringroad Selatan, Kragilan, Tamanan, Kec. Banguntapan, Bantul, Daerah Istimewa Yogyakarta 55191, Indonesia

^{**} Department of Chemical Engineering, Faculty of Engineering, Universitas Gadjah Mada, Jl. Grafika No. 2, Kampus UGM, Yogyakarta, 55281, Indonesia

(sitijamilatun@che.uad.ac.id, endahsulistiawati@che.uad.ac.id, shinta.amelia@che.uad.ac.id, abudiman@ugm.ac.id)

[‡] Corresponding Author; first author, Tel: +62 0274-563515 ext 4211,

Fax: +62 0274-564604, sitijamilatun@che.uad.ac.id

Received: 04.10.2020 Accepted: 29.10.2020

Abstract- *Spirulina platensis* residue (SPR) pyrolysis can produce tar fuels. The use of a silica-alumina catalyst will improve fuel quality by reducing oxygenate compounds. The kinetics of non-catalytic reactions and SPR catalytic pyrolysis have studied using the primary and secondary cracking model approaches. Data obtained from a fixed-bed reactor at 300-600 °C is the weight of tar each time, weight gas, and char gained at the end of the process. A pyrolysis scheme is made to determine the reaction of product formation with primary and secondary cracking models. From the calculation of pyrolysis without catalyst, the activation energy obtained in primary cracking is E_1 , E_2 , E_3 , while for secondary cracking is E_4 and E_5 . The optimum condition in primary cracking is E_3 . The SPR reaction becomes char ($B \rightarrow C(1)$) with the lowest activation energy of 15.418 kJ/mol (k_3 in the range of $0.1044-0.0279 \text{ sec}^{-1}$), while for secondary cracking, the tar (1) reaction becomes char ($T(1) \rightarrow C(2)$) of 15.151 kJ/mol (k_5 in the range $1.80 \cdot 10^{-6}-5.48 \cdot 10^{-7} \text{ sec}^{-1}$). In pyrolysis with silica-alumina catalyst (10, 20 and 40 wt.%), The more catalyst used, the smaller the E_a , and optimal for primary cracking in the use of catalyst 40 wt.%, i.e., in the decomposition of SPR to char, E_3 of 3.004 kJ/mol (k_3 in the range $0.0616-0.0528 \text{ sec}^{-1}$). For secondary cracking in the use of catalysts 10, 20, and 40 %, E_4 and E_5 are relatively high, i.e., in the range of 40.855-52.085 kJ/mol (k_4 and k_5 in the range $3.89 \cdot 10^{-6}-8.40 \cdot 10^{-7} \text{ sec}^{-1}$).

Keywords: *Spirulina platensis* residue; silica-alumina; fixed-bed reactor; primary and secondary cracking models; activation energy.

1. Introduction

Pyrolysis of *Spirulina platensis* residue (SPR) produces tar, gas, and char [1-5]. Until now, pyrolysis technology is still exciting to discuss because of its inexpensive and straightforward technique. Unfortunately, tar products cannot be applied as fuel because the oxygenate compounds are high enough to cause corrosion in engines [6-8]. Therefore it is necessary to find a solution to reduce the content of

oxygenated compounds in tar while knowing the composition of the product yield, one of which is catalytic pyrolysis using silica-alumina in a fixed-bed reactor. The use of silica-alumina can reduce the average O/C ratio from non-catalytic to catalytic pyrolysis SPR by 69.66 %, i.e., from 0.55 to 0.155 [6].

For this reason, it is essential to study the kinetics and the mechanism of the catalytic pyrolysis reaction with silica-alumina for the development of quality fuels. For this reason,

it is crucial to study the kinetics and the mechanism of the catalytic pyrolysis reaction with silica-alumina for the development of quality fuels. The reaction mechanism and cracking modeling are needed to determine each product formation; then, it can predict which product is the most easily formed [9-10]. The ultimate goal is to use the data obtained to design fuel plants from commercial-scale SPR biomass.

Calculation of reaction kinetics determines the activation energy and reaction speed constants generally obtained from Thermogravimetric analysis data [10]. Kinetics study of *Chlorella vulgaris* [6]; pyrolysis calculated by the isoconversional method model by Flynn Wall Ozawa (FWO) at [6] Kissinger Akahira Sunose (KAS) with the catalysts of CaO, MgO, K₂CO₃, BaCO₃, and Na₂CO₃, average activation in the range of 99.60-134.05 kJ/mol from without catalysts 109.7 kJ/mol [11]. Calculations with the Coats-Redfern integral method by Balasundram et al., 2017 [12] with a rice husk catalyst, can reduce the activation energy from without a catalyst 49.78 to 45.24 kJ/mol. *Spirulina platensis* residue pyrolysis kinetics study using Thermogravimetric Analyzer, which was completed with the least-squares method, obtained activation energy (E_a) for each heating rate of 10, 20, 30, 40, and 50 °C/min was 35.455, 41.102, 45.702, 47.892 and 47.562 kJ/mol [13].

The study of reaction kinetics by modeling the data obtained from fixed-bed reactors is still small compared to the thermogravimetric analysis. Therefore, the study of reaction kinetics with a fixed-bed reactors database without catalysts and catalysts is needed to obtain the activation energy value and constant reaction speed. Biomass pyrolysis through a series of competitive reactions is involved, while the exact mechanism is still unknown. For this reason, kinetic schemes that are widely applicable still require a more in-depth study [14-20].

This study studies silica-alumina catalysts' effect on the kinetics of the residual *Spirulina platensis* reaction in a fixed-bed reactor. Kinetics solution using the primary and secondary cracking model approaches. The reaction mechanism used for the primary and secondary models is explained in Figure 1.

1.1. Secondary tar cracking model

The primary and secondary tar cracking reaction mechanism proposed by Prakash and Karunanti, 2008 [14], is shown in Figure 1.

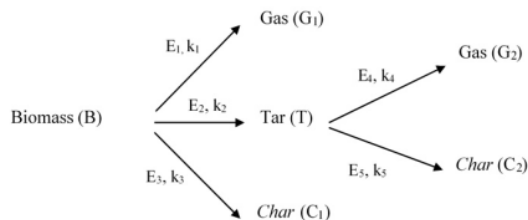


Figure 1. Primary and Secondary cracking model [14]

1.2. Model formulation

The kinetic scheme in Figure 1 illustrates the thermal decomposition of primary pyrolysis, which is biomass (B) to

gas (G₁), tar (T), and char (C₁). Secondary pyrolysis is tar (T₁) decomposed into char (C₂) and gas (G₂).

This model based on the following assumptions [14-16]:

1. The solid is constant and is not affected by temperature.
2. Heat transfer takes place by conduction on solids. Thermal conductivity and heat capacity is constant.
3. The biomass's pyrolysis speed increases as temperature increases, while the reaction rate constant (k) follows Arrhenius's law.
4. The reaction speed is first order, and the reaction is endothermic, with primary and secondary pyrolysis processes.
5. There is no temperature gradient at the pore center.
6. At $r = 0$ of solid particles, $[\partial T / \partial r]_{(r=0)} = 0$

$$\frac{\partial x_B}{\partial t} = -(k_1 + k_2 + k_3)X_B \quad (1)$$

$$\frac{\partial x_T}{\partial t} = k_2X_B - (k_4 + k_5)X_T \quad (2)$$

$$\frac{\partial x_C}{\partial t} = k_3X_B + k_5X_T \quad (3)$$

$$\frac{\partial x_G}{\partial t} = k_1X_B + k_4X_T \quad (4)$$

Pyrolysis is done with isothermal way, so the Arrhenius equation approximates k:

$$k = A \exp \left[\left(\frac{-E}{RT} \right) \right] \quad (5)$$

Notation B, T, C, and G are biomass (SPR), tar, char, and gas. The initial condition for Equation (1-5) is:

$$t = 0, X_B = X_{B0} = 1, X_{C0} = X_{G0} = X_{T0} = 0 \quad (6)$$

The value k of each reaction follows the Arrhenius equation, as in Equation 5. There are four ordinal differential equations (Equations 1-4) that can be solved simultaneously by numerical methods. The obstacle in completing this model is that it cannot separate the biomass and charcoal, and the weight is observed.

Changes in biomass weight in the reactor could not find because the remaining biomass with char that formed each time mixed so that the amount could not observe. The data that can see from experiments is the weight of tar created each time; therefore, the secondary cracking model can complete in the following way.

$$W_{B0} = W_{C\text{ end}} + W_{T\text{ end}} + W_{G\text{ end}} \quad (7)$$

Or in weight fraction,

$$X_{B0} = 1 = X_{T\text{ end}} + X_{C\text{ end}} + X_{G\text{ end}} \quad (8)$$

W_{B0} , $W_{C\text{ end}}$, $W_{T\text{ end}}$, and $W_{G\text{ end}}$ notations are the initial SPR biomass's weight, the final char weight, the final tar weight, and the last gas weight. Each notation is the initial SPR biomass weight fraction, the final char weight fraction, the final tar weight fraction, and the ultimate gas weight fraction.

Values k_1 , k_2 , k_3 , k_4 , and k_5 , are tested to obtain the minimum average error.

$$Error_{rate\ relatif} = \frac{\sum[(X_G)_{count} - (X_G)_{data}] + \sum[(X_T)_{hitungan} - (X_T)_{data}] + \sum[(X_C)_{hitungan} - (X_C)_{data}]}{(9)}$$

The flow of completion from the model can see in Figure 2.

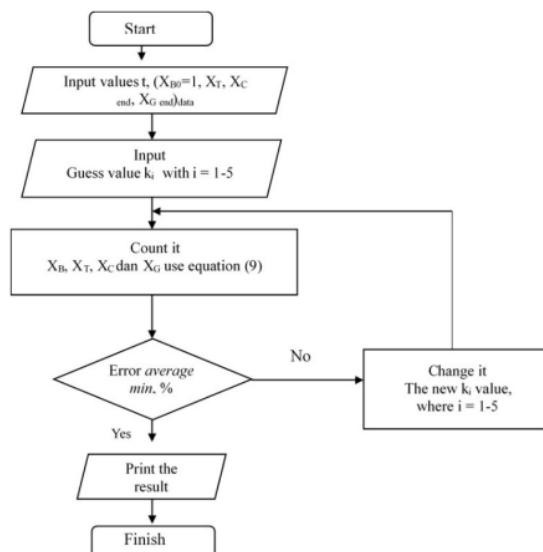


Figure 2. Flow chart of mathematical equation primary and secondary models

2. Methodology

2.1 Materials

Dry *Spirulina platensis* residue (SPR) obtained from solid residue of *Spirulina platensis* (SP) extraction with solvent. The ultimate, proximate, and Higher Heating Value (HHV) analyzed samples from SPR. Laboratorium Pangan dan Hasil ¹¹anian, Departemen Teknologi Pertanian, and Laboratorium Pangan dan Gizi, Pusat Antar Universitas (PAU) UGM, carried out the proximate analysis. As for the ultimate, it performed at Laboratorium Pengujian, Puslitbang Tekmira, Bandung [4,8,9,13]. The results of sample testing shown in Table 1.

From PT. Pertamina Balongan obtained the silica-alumina catalyst powder. Use of catalyst in pellets made by mixing 95 wt.% silica-alumina with 5 (five) wt.% Kaolin, then adding enough distilled water. The mixture is mixed until homogeneous and then printed with a 4 mm pellet diameter and 6 mm height. Silica alumina pellets dried in the sun for 2 (two) days, and then heating is carried out in a furnace at 500 °C for 2 (two) hours. The Laboratorium Pengujian dan Penelitian Terpadu ⁴ (LPPT), UGM, conducted the silica-alumina catalyst analyzed by SEM-EDX (Scanning Electron Microscope – Energy Dispersive X-ray) and BET [6-9,20]. The International Frontier Division, Dept. Transdisciplinary

Science and Technology School of Environmental and Society, Tokyo Institute of Technology, Japan carried out X-ray fluorescence (XRF).

2.2. Methods

SPR microalgae ⁷rolysis experiments carried out with and without catalyst in a fixed-bed reactor made of stainless steel with dimensions: inner diameter = 40 mm, outer width = 44 mm, and height = 600 ⁹ [12-15]. The reactor is equipped with a heater. The tool diagram for the fixed-bed reactor system is presented in Figure 3 [4,6-9].

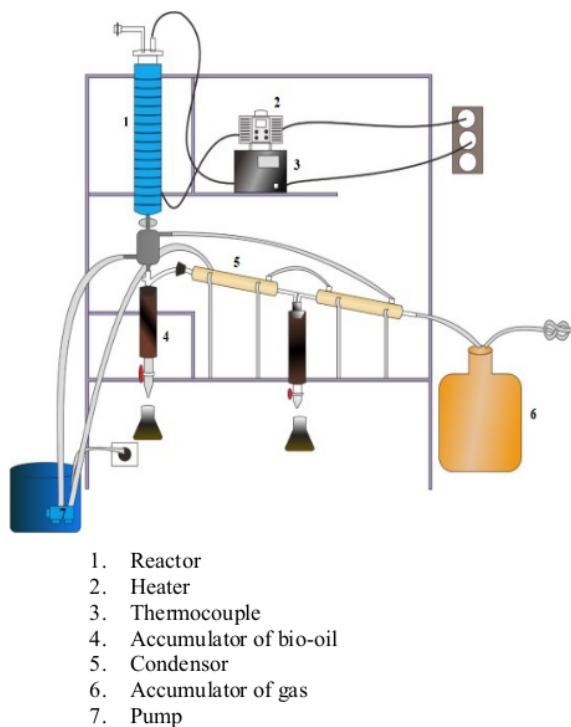


Figure 3. Series of experimental devices

Fifty (50) g ⁵R was put into the reactor, tightly closed, and heated. The reactor was heated externally by an electric furnace, and the temperature-controlled by a NiCr-Ni thermocouple placed outside the furnace. The tested sample was heated with a constant heating rate from room temperature to the desired temperature and kept steady for 1 hour. The liquid product is coming out of the condenser collected in an accumulator, and gas production is measured. Liquid products (tar) separated by decantation. After the experiment does, the number of solids (char) left behind was taken and weighed. The total liquid products (bio-oil and water phase), gas, and gas are calculated by the equation [4,6-9,13,15-21]:

$$Y_L = \frac{W_L}{W_M} 100\% \quad (10)$$

$$Y_{B0} = \frac{W_{B0}}{W_M} 100\% \quad (11)$$

$$Y_A = \frac{W_A}{W_M} 100\% \quad (12)$$

$$Y_C = \frac{W_C}{W_M} 100\% \quad (13)$$

$$Y_G = 1 - (Y_L + Y_C) \quad (14)$$

In this case, Y_L , Y_{B0} , Y_A , Y_C , and Y_G notations are liquid product yields, bio-oil, water phase, char, and gas. Meanwhile, W_M , W_L , W_A , W_{B0} , and W_C are the initial SPR weight, the liquid product's value, the water phase, bio-oil, and char.

3. Results

3.1. Characteristics of *Spirulina platensis* residue (SPR)

The result of SPR proximate, ultimate, and HHV analysis of the study results are presented in Table 1.

Table 1. Characteristics of *Spirulina platensis* residue (SPR)[4].

Component	SPR
Composition analysis (%)	
Lipid	0.09
Carbohydrate	38.51
Protein	49.60
Proximate analysis (%)	
Moisture	9.99
Ash	8.93
Volatiles	68.31
Fixed carbon	12.77
Ultimate analysis (%)	
Sulfur	0.55
Carbon	41.36
Hydrogen	6.60
Nitrogen	7.17
Oxygen	35.33
O/C, the molar ratio	0.64

Based on Table 1 can seem that SPR has a composition; component C is 41.36 wt.%, H is 6.60 wt.%, and N is 7.17 wt.%, O is 35.33 wt.%. Meanwhile, for the proximate analysis, lipid at SPR 0.09 wt.%, carbohydrate is 25.59 wt.%, and protein is 49.60 wt.% [12]. The molar ratio of O/C is 0.64 [4].

The UGM conducted a silica-alumina catalyst analyzed by SEM-EDX (Scanning Electron Microscope – Energy Dispersive X-ray) and BET at the Laboratorium Pengujian dan Penelitian Terapan (LPPT), UGM. SEM-EDX yields are weight percent C, O, Al, and Si respectively 8.41, 55.78, 24.64, and 11.17 %. Whereas from BET for surface area and pore diameter is 240.533 m²/gram and 3.3 nm. XRF microscopy analyzes obtained by weight percent SiO₂, Al₂O₃ is 60.28 and 35.25 wt.%,

3.2. The yield of SPR pyrolysis products with fixed-bed reactors

Figure 4 shows that the SPR non-catalytic and catalytic pyrolysis obtained product yields calculated by Equation (10-14).

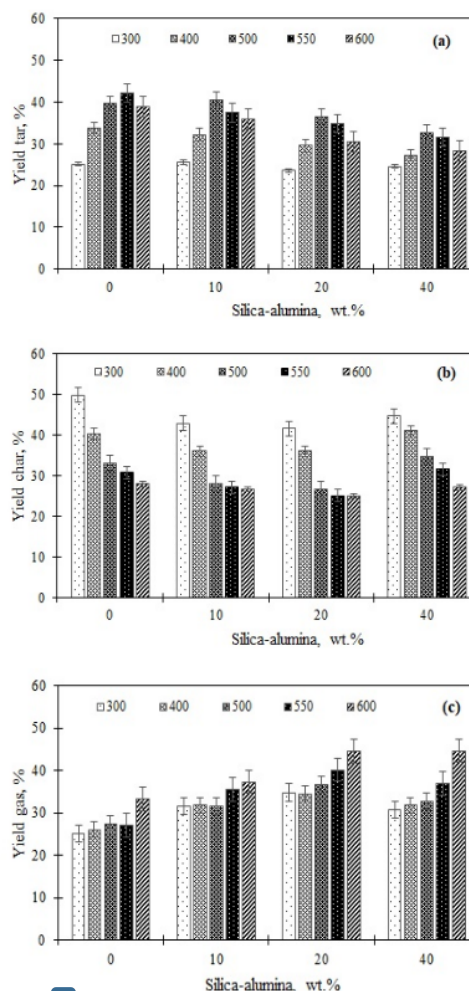


Figure 4. Effect of temperature on product yields with non-catalytic and catalytic pyrolysis in fixed-bed reactors: (a) Tar, (b) Char and (c) Gas

Figure 4a shows that the higher the pyrolysis temperature for non-catalytic and catalytic pyrolysis, the tar yield will rise to the optimum temperature, then decrease again. This phenomenon is because secondary cracking occurs from tar formed in primary cracking; tar decomposes into gas and char. The optimum temperature and yield formed for non-catalytic and silica-alumina use of 0, 10, 20, and 40 % are 550 °C (42.01 %), 500 °C (40.55 %), 500 °C (36.55 %), and 500 °C (32.55 %). The use of silica-alumina catalysts reduces tar yield; this phenomenon is caused by silica-alumina being able to activate secondary cracking by forming new reaction paths. The tar formed in primary cracking will decompose to form gas with a very significant and slight addition of char, as shown in Figures 4b and 4c. In Figure 4c, we can see the optimum addition of gas at the use of a catalyst of 20 %. The range of gas without catalyst yields and the use of catalysts 0, 10, 20, and 40 % are 25.03-33.28, 31.52-37.34, 34.78-44.45, and 30.71-44.67 %.

3.3. Effect of temperature and amount of silica-alumina on the O/C ratio

The O/C ratio can illustrate the fuel quality, the impact of heat, and the amount of silica-alumina shown in Figure 5.

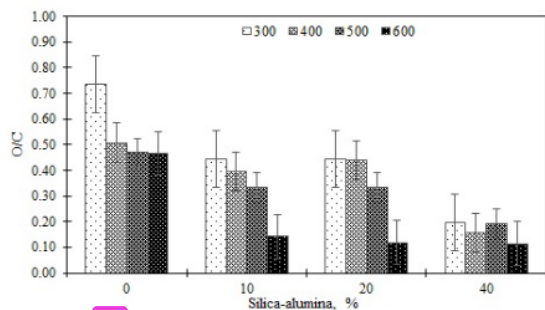


Figure 5. Effect of temperature and use of catalyst on O/C bio-oil SPR

The figure shows that the higher the temperature for non-catalytic and catalytic pyrolysis has the same tendency, namely the decrease in the O/C ratio. The silica-alumina use can reduce the O/C ratio from 0.47-0.74 for non-catalytic to 0.11-0.20 at optimum silica-alumina conditions by 40 %. As a comparison of fuel quality by referring to the O/C ratio, for

petroleum oil, bio-oil from wood, *C. Protothecoides*, SPR without (0 %) and with catalysts (10, 20 and 30 %) pyrolysis obtained O/C average are 0.553 0.330, 0.340, and 0.155, respectively [13]. The use of silica-alumina catalysts is very significant to reduce the content of oxygenate compounds [13,21].

3.4. Model Test with Fixed-bed Reactor

3.4.1. Non-Catalytic Pyrolysis

The two-stage pyrolysis model involved primary and secondary tar crackings, while the reaction scheme can see in Figure 6.

Figure 6 shows SPR weight fraction and SPR pyrolysis products at a temperature of 300 °C from the experiment (X_{Data}) and calculation results (X_{Model}) at various times. From the picture, it can see the data that can observe from the experimental results at 300 °C is the weight fraction of tar (X_{Tar}) each time, while char (X_{Char}) and gas (X_{Gas}) can only calculate at the end of the experiment. SPR Fraction (X_{SPR}) is only known at the beginning of the investigation. In massive operations, SPR and char cannot observe every time because they are mixed in solids. For this reason, Equation 8 becomes a reference in completing this model.

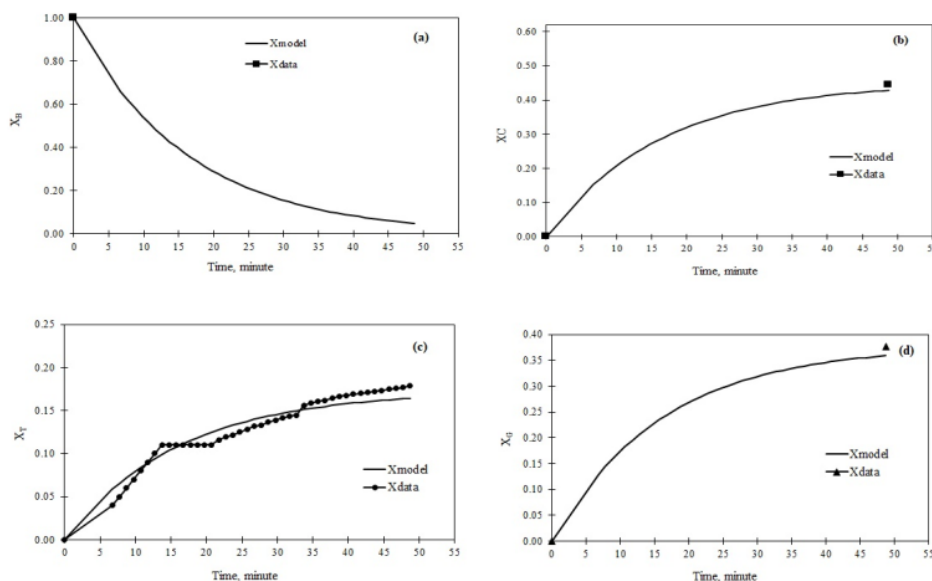


Figure 6. Relationship between pyrolysis time (minutes) and weight fraction (X_{Data} and X_{Model}) at 300 °C: (a) SPR; (b) Tar; (c) Char and (d) Gas

Figure 6 shows SPR weight fraction and SPR pyrolysis products at a temperature of 300 °C from the experiment (X_{Data}) and calculation results (X_{Model}) at various times. From the picture, it can see the data that can observe from the experimental results at 300 °C is the weight fraction of tar

(X_{Tar}) each time, while char (X_{Char}) and gas (X_{Gas}) can only calculate at the end of the experiment. SPR fraction (X_{SPR}) is only known at the beginning of the investigation. In massive operations, SPR and char cannot observe every time because

they are mixed in solids. For this reason, Equation 8 becomes a reference in completing this model.

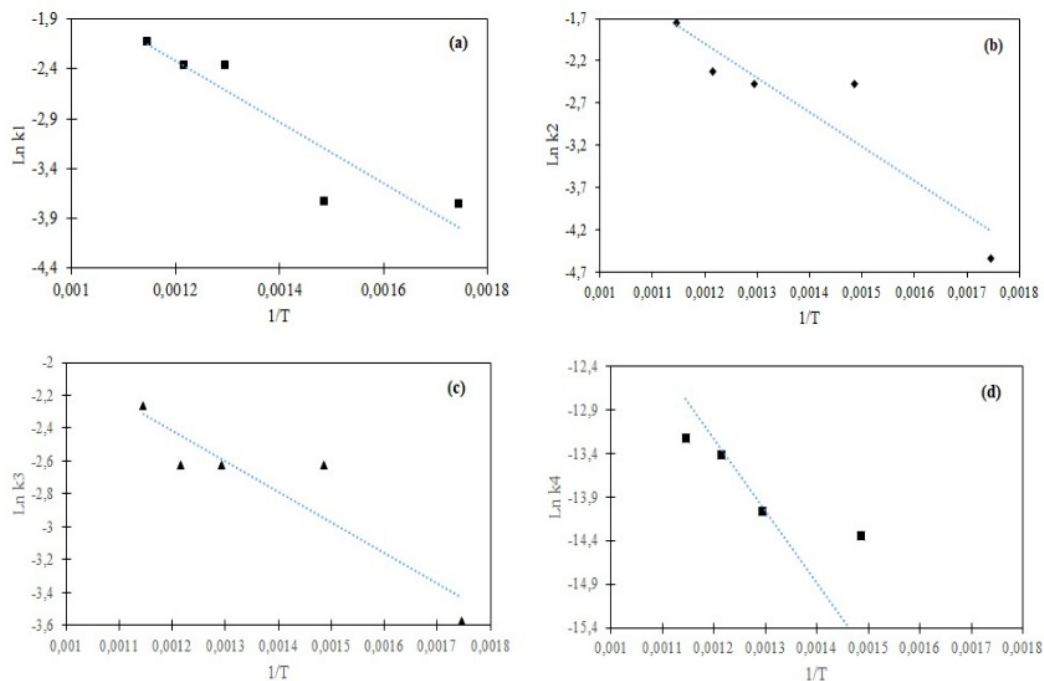
The model's weight fraction is calculated by entering k_i for $i = 1-5$ in equation (1-4) until value $X_{total}=1$ (Equation 8) with

an error between X_{Data} , and X_{Model} that has the smallest value. After obtaining k_i for a temperature of 300-600 °C, k_i was used to calculate A_i and E_i , where $i = 1-5$. The values of k_1 , k_2 , k_3 , k_4 , and k_5 at a temperature of 300-600 °C are presented in Table 2.

Table 2. The values of k_1 , k_2 , k_3 , k_4 , and k_5 at temperatures of 300-600 °C in pyrolysis

T, °C	$k_1(\text{sec}^{-1})$	$k_2(\text{sec}^{-1})$	$k_3(\text{sec}^{-1})$	$k_4(\text{sec}^{-1})$	$k_5(\text{sec}^{-1})$	Error, %
300	0.0237	0.0107	0.0279	$5.48 \cdot 10^{-7}$	$5.48 \cdot 10^{-7}$	5.45
400	0.0240	0.0839	0.0722	$5.88 \cdot 10^{-7}$	$6.42 \cdot 10^{-7}$	8.17
500	0.0940	0.0839	0.0722	$7.78 \cdot 10^{-7}$	$7.99 \cdot 10^{-7}$	8.91
550	0.0940	0.0984	0.0722	$1.49 \cdot 10^{-6}$	$1.39 \cdot 10^{-6}$	7.10
600	0.1201	0.1743	0.1044	$1.80 \cdot 10^{-6}$	$1.70 \cdot 10^{-6}$	4.12

Each temperature obtained the values of k_1 , k_2 , k_3 , k_4 , and k_5 , a relationship made between $1/T$ and $\ln k_i$, where $i = 1-5$. This relationship is illustrated in Figure 7.



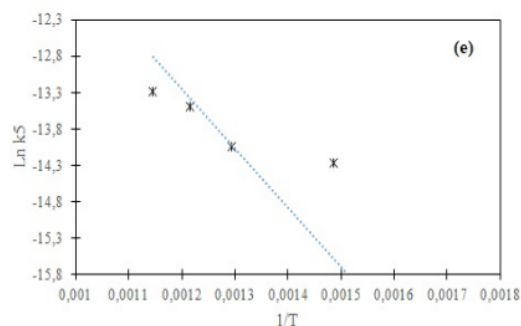


Figure 7. Relationship between $1/T$ and $\ln k$: (a) $\ln k_1$, (b) $\ln k_2$, (c) $\ln k_3$, (d) $\ln k_4$ and (e) $\ln k_5$

Furthermore, from Figure 7, values A_1 - A_5 and E_1 - E_5 will be obtained as outlined in Table 3.

Table 3. Value of A_i and E_i in the primary and secondary tar cracking model

Reaction	A_i	$E_i(\text{J/mol})$
$k_1, B \rightarrow G(1)$	3.8574	25,414.60
$k_2, B \rightarrow T(1)$	18.0366	33,778.51
$k_3, B \rightarrow C(1)$	0.8301	15,418.08
$k_4, T(1) \rightarrow G(2)$	$1.377 \cdot 10^{-5}$	16,283.77
$k_5, T(1) \rightarrow C(2)$	$1.138 \cdot 10^{-5}$	15,150.82

Table 3 shows that the sequence of activation energies of the greatest is $B \rightarrow T(1)$, $B \rightarrow G(1)$, $T(1) \rightarrow G(2)$, $B \rightarrow C(1)$, and $T(1) \rightarrow C(2)$. This value can interpret that it takes the most energy to convert biomass into Tar (1) or intermediate

product tar. The benefits of E_1 - E_5 prove that secondary cracking does occur, and the reaction of Tar (1) turns to Gas (2) and Char (2).

3.4.2. Catalytic Pyrolysis

Table 4 shows that the higher the pyrolysis temperature for all catalyst uses, the greater the k_1 - k_5 . The higher the heat of the reaction, the more energy the molecules get. The energy obtained is used to increase molecular motion's kinetic energy, increasing collisions' frequency between particles and catalysts. Partial energy collisions use to break existing bonds and form new relationships. This phenomenon encourages chemical reactions, where more collisions increase reaction speed. The catalyst can reduce the activation energy with the same power, the number of accidents that work is more, and the reaction rate is faster.

Table 4. Values of k_1 , k_2 , k_3 , k_4 , and k_5 at temperatures of 400-600 °C in pyrolysis with catalyst

Catalyst 10						
$T, ^\circ\text{C}$	$k_1(\text{sec}^{-1})$	$k_2(\text{sec}^{-1})$	$k_3(\text{sec}^{-1})$	$k_4(\text{sec}^{-1})$	$k_5(\text{sec}^{-1})$	Error, %
400	0.0489	0.0449	0.0468	$6.45 \cdot 10^{-7}$	$6.45 \cdot 10^{-7}$	7.49
450	0.0646	0.0499	0.0469	$7.57 \cdot 10^{-7}$	$7.24 \cdot 10^{-7}$	3.74
500	0.0994	0.0641	0.0601	$8.77 \cdot 10^{-7}$	$8.60 \cdot 10^{-7}$	1.80
600	0.1670	0.1024	0.0911	$4.55 \cdot 10^{-6}$	$4.55 \cdot 10^{-6}$	2.14
Catalyst 20						
$T, ^\circ\text{C}$	$k_1(\text{sec}^{-1})$	$k_2(\text{sec}^{-1})$	$k_3(\text{sec}^{-1})$	$k_4(\text{sec}^{-1})$	$k_5(\text{sec}^{-1})$	Error, %
400	0.0520	0.0476	0.0469	$6.88 \cdot 10^{-7}$	$6.84 \cdot 10^{-7}$	5.92
450	0.0520	0.0479	0.0469	$8.00 \cdot 10^{-7}$	$7.94 \cdot 10^{-7}$	7.07
500	0.0790	0.0704	0.0543	$8.91 \cdot 10^{-7}$	$8.88 \cdot 10^{-7}$	4.04
600	0.1581	0.0953	0.0735	$6.04 \cdot 10^{-6}$	$6.04 \cdot 10^{-6}$	0.66
Catalyst 40						
$T, ^\circ\text{C}$	$k_1(\text{sec}^{-1})$	$k_2(\text{sec}^{-1})$	$k_3(\text{sec}^{-1})$	$k_4(\text{sec}^{-1})$	$k_5(\text{sec}^{-1})$	Error, %
400	0.0537	0.0449	0.0528	$8.40 \cdot 10^{-7}$	$8.35 \cdot 10^{-7}$	10.69
450	0.0546	0.0470	0.0528	$9.16 \cdot 10^{-7}$	$9.15 \cdot 10^{-7}$	11.86
500	0.0547	0.0611	0.0528	$9.56 \cdot 10^{-7}$	$9.54 \cdot 10^{-7}$	8.17
600	0.0964	0.0925	0.0616	$3.89 \cdot 10^{-6}$	$3.79 \cdot 10^{-6}$	1.62

The data of k_1 - k_5 for pyrolysis with catalysts (10, 20, and 40 %) were used to calculate A_1 - A_5 and E_1 - E_5 , presented in Table 5. From the table, it can seem that the more catalysts used, the smaller E_1 , E_2 , E_3 , E_4 , and E_5 . This value can interpret that with the use of catalysts, the lower the activation energy, the more efficiently the reaction occurs. It is optimum at the use of the catalyst 40 wt.% at primary cracking, which is in the decomposition of SPR to gas, tar, and char are E_1 (14.03 kJ/mol), E_2 (17.89 KJ/mol), and E_3 (3.00 kJ/mol), respectively.

In the use of catalysts, 10 % with 400-600 °C the k_1 , k_2 dan k_3 are obtained in the range 0.0489-0.1670, 0.0449-0.1024, and 0.0468-0.0911 sec⁻¹, respectively. Furthermore, for catalyst 20 % is obtained 0.0520-0.1581, 0.0476-0.0953, and 0.0469-0.0735 sec⁻¹, respectively. The use of a catalyst 40 % is obtained from 0.0537-0.0964, 0.0449-0.0925, and 0.0528-0.0616 sec⁻¹, respectively.

Table 5. Values of A_1 - A_5 and E_1 - E_5 (kJ/mol) on pyrolysis with catalysts

Catalyst (%)	E_1 (kJ/mol)	A_1	E_2 (kJ/mol)	A_2	E_3 (kJ/mol)	A_3	E_4 (kJ/mol)	A_4	E_5 (kJ/mol)	A_5
0	21.79	1.17	25.70	2.63	3.58	0.07	22.71	3.10^{-5}	22.55	3.10^{-5}
10	30.00	10.13	18.18	1.13	14.61	0.60	52.09	0.005	46.64	0.002
20	27.91	6.53	17.08	0.94	12.32	0.40	51.63	0.005	51.82	0.005
40	14.03	0.59	17.89	1.02	3.00	0.09	41.22	0.001	40.86	0.001

4. Conclusions

Spirulina platensis residue (SPR) with shallow lipid content (0.09 wt.%), protein content (49.60 wt.%), and carbohydrate (38.51 wt.%) high enough to be pyrolyzed with and without catalyst (silica-alumina) produces bio-oil, water phase, gas, and char. With the primary and secondary tar cracking model, data obtained from experiments with fixed-bed reactors using SPR at 300-600 °C. Based on the calculation of pyrolysis without catalyst, the activation energy obtained in primary cracking is $E_1(B \rightarrow G(1))$, $E_2(B \rightarrow T(1))$, $E_3(B \rightarrow C(1))$. In contrast, for secondary cracking, it is $E_4(T(1) \rightarrow G(2))$ and $E_5(T(1) \rightarrow C(2))$. The successive activation energy values are 25.425, 33.779, 15.418, 16.284, and 15.151 kJ/mol. The easiest to react in primary cracking is SPR to char with the lowest activation energy of 15.151 kJ/mol. Still, in the secondary cracking, the activation energy for the reaction of tar, T(1) to gas (G(2)), and char (C(2)) is almost the same value, 16.284 and 15.151 kJ/mol. With the secondary tar cracking model on pyrolysis with various catalysts (10, 20, and 40 wt.%), the more catalysts used, the smaller E_a . It is optimum at the use of the catalyst 40 wt.%, which is in the decomposition of SPR to char, E_3 (3.00 kJ/mol).

Acknowledgment

The researcher would like to thank the internal research funding assistance through the Lembaga Penelitian dan pengabdian Masyarakat (LPPM) Ahmad Dahlan University Yogyakarta with a contract number: PD-237/SP3/LPPM-UAD/2020.

References

- [1] M. Aziz, T. Oda, and T. Kashiwagi, "Novel power generation from microalgae: Application of different gasification technologies," International Conference on Renewable Energy Research and Applications (ICRERA), Palermo, pp. 745-749; doi: 10.1109/ICRERA. 2015. 7418510. 22-25 November 2015.
- [2] F. Banda, D. Giudici, S. Quegan, and K. Scipal, "The Retrieval Concept of the Biomass Forest Biomass Prototype Processor," Published in IGARSS 2018 - 2018 IEEE International Geoscience and Remote Sensing Symposium- IEEE Conference Publication, 05 November 2018, DOI: 10.1109/IGARSS.2018.8518434.
- [3] K. Shi, S. Shao, Q. Huang, X. Liang, L. Jiang, and Y. Li, "Review of catalytic pyrolysis of biomass for bio-oil," Published in 2011 International Conference on Materials for Renewable Energy & Environment-IEEE Conference Publication, pp. 317-321, 27 June 2011 DOI: 10.1109/ICMREE.2011.5930821.
- [4] K.E. Okedu, and M. Al-Hashmi, "Assessment of the Cost of various Renewable Energy Systems to Provide Power for a Small Community: Case of Bukha, Oman," International Journal of Smart Grid- ijSmartGrid, Vol.2, No.3, pp. 172-182, September 2018.
- [5] K. Ahmadi, M. Fujiwara, Y. Nakamura, K. Sato, H. Takami, K. Ahmadi, M. Fujiwara, Y. Nakamura, K. Sato, and H. Takami, "ILQ Optimal Voltage Control for Biomass Free-Piston Stirling Engine Generator System", International Journal of Smart Grid- ijSmartGrid, Vol.4, No.1, pp. 38-43, March 2020.
- [6] S. Jamilatun, Budhijanto, Rochmadi, A. Yuliestyan, A. Budiman, "Valuable Chemicals Derived from Pyrolysis Liquid Products of *Spirulina platensis* residue." Indones. J. Chem., Vol. 19, No. 3, pp. 703 – 711, 2019.
- [7] S. Jamilatun, Budhijanto, Rochmadi, A. Yuliestyan, A. Budiman, "Comparative Analysis Between Pyrolysis Products of *Spirulina platensis* Biomass and Its Residues." Int. J. Renew. Energy Dev., Vol. 8, No. 2, pp. 113 – 140, 2019.
- [8] S. Jamilatun, A. Budiman, H. Anggorowati, A. Yuliestyan, Y. Surya Pradana, Budhijanto, Rochmadi, "Ex-Situ

- Catalytic Upgrading of *Spirulina platensis* residue Oil Using Silica Alumina Catalyst." International Journal of Renewable Energy Research. Vol. 9, No. 4, pp. 1733–1740, 2019.
- [9] M. Oku, T. Sakoda, N. Hayashi, and D. Tashima, "Basic characteristics of a heat and electricity combined generation system using biomass fuel," International Conference on Renewable Energy Research and Application (ICRERA), Milwaukee, WI, 2014, pp. 222-228; doi:10.1109/ICRERA. 2014 .7016560. 19-22 Oktober 2014.
- [10] C. Di Blasi, "Analysis of convection and secondary reaction effects within porous solid fuels undergoing pyrolysis. Combust. Sci. Technol., Vol. 90, pp. 315–340, 1993.
- [11] Q. Xu, X. Ma, Z. Yu, Z. Cai, "A kinetic study on the effects of alkaline earth and alkali metal compounds for catalytic pyrolysis of microalgae using thermogravimetry," Applied Thermal Engineering 73, 357-361, 2014.
- [12] V. Balasundram, N. Ibrahim, R.Md. Kasmani, M.K. Abd. Hamid, R. Isha, H. Hasbullah, and R.R. Ali, "Thermogravimetric catalytic pyrolysis and kinetic studies of coconut copra and rice husk for maximum possible production of pyrolysis oil," Journal of Cleaner Production 167, 218-228, 2017.
- [13] S. Jamilatun, Budhijanto, Rochmadi, A. Budiman, "Thermal Decomposition and Kinetic Studies of Pyrolysis of *Spirulina platensis* residue." International Journal of Renewable Energy Development, Vol. 6, No. 3, pp. 193–201, 2017.
- [14] N. Prakash, T. Karunanithi, "Kinetic modeling in biomass pyrolysis – A Review." J. Appl. Sci. Res., Vol. 4, No. 12, pp. 1627-1636, 2008.
- [15] A. Anca-Counce, R. Mehrabian, I. Scharler, Obernberger, "Kinetic scheme of biomass pyrolysis considering secondary charring reactions." Energy Conversion and Management, Vol. 87, pp. 687–696, 2014.
- [16] B.M.E. Chagas, C. Dorado, M.J. Serapiglia, C.A. Mullen, A.A. Boateng, M.A.F. Melo, C.H. Ataíde, "Catalytic pyrolysis-GC/MS of *Spirulina*: Evaluation of a highly proteinaceous biomass source for the production of fuels and chemicals," Fuel, Vol. 179, pp. 124–134, 2016.
- [17] A. Demirbas, M.F. Demirbas, "Importance of algae oil as a source of biodiesel," Energy Conversion, and Management. Vol. 52, pp. 163-170, 2011.
- [18] A. Sharma, V. Pareek, D. Zhang, "Biomass pyrolysis—A review of modeling, process parameters and catalytic studies", Vol. 50, pp. 1081-1096, 2015.
- [19] M. Aziz, T. Oda, T. Mitani, A. Uetsuji, and T. Kashiwagi, "Combined hydrogen production and power generation from microalgae," International Conference on Renewable Energy Research and Applications (ICRERA), Palermo, pp. 923-927; doi:10.1109/ICRERA. 7418544. 22-25 November 2015.
- [20] S.J. Ojolo, C.A. Osheku, M.G. Sobamowo, "Analytical investigations of kinetic and heat transfer in the slow pyrolysis of a biomass particle." Int. J. Renew. Dev., Vol. 2, No. 2, pp.105-115, 2013.
- [21] S. Jamilatun, Budhijanto, Rochmadi, J-I. Hayashi and A. Budiman "Catalytic pyrolysis of *Spirulina platensis* residue (SPR): Thermochemical behavior and kinetics," International Journal of Technology, 11(3), pp. 522-531, 2020.

8. IJRER

ORIGINALITY REPORT

9%

SIMILARITY INDEX

PRIMARY SOURCES

1	ijrer.org Internet	112 words — 3%
2	openchemicalengineeringjournal.com Internet	48 words — 1%
3	ejournal.undip.ac.id Internet	48 words — 1%
4	ejournal.uin-malang.ac.id Internet	23 words — 1%
5	link.springer.com Internet	21 words — < 1%
6	Qing Xu, Xiaoqian Ma, Zhaosheng Yu, Zilin Cai. "A kinetic study on the effects of alkaline earth and alkali metal compounds for catalytic pyrolysis of microalgae using thermogravimetry", Applied Thermal Engineering, 2014 Crossref	20 words — < 1%
7	Aysu, T.. "The Effect of Boron Minerals on Pyrolysis of Common Reed (Phragmites australis) for Producing Bio-oils", Energy Sources Part A Recovery Utilization and Environmental Effects, 2014. Crossref	17 words — < 1%
8	M. Auta, L.M. Ern, B.H. Hameed. "Fixed-bed catalytic and non-catalytic empty fruit bunch biomass pyrolysis", Journal of Analytical and Applied Pyrolysis, 2014 Crossref	16 words — < 1%

9	Halil Durak. "Thermochemical conversion of <i>Phellinus pomaceus</i> via supercritical fluid extraction and pyrolysis processes", Energy Conversion and Management, 2015 Crossref	10 words — < 1%
10	Kecheng Li. "Sample Contamination in Analysis of Wood Pulp Fibers with X-ray Photoelectron Spectroscopy", Journal of Wood Chemistry and Technology, 1/1/2005 Crossref	9 words — < 1%
11	javaneseasli.blogspot.com Internet	9 words — < 1%
12	Vekes Balasundram, Norazana Ibrahim, Rafiziana Md Kasmani, Mohd. Kamaruddin Abd. Hamid et al. "Thermogravimetric catalytic pyrolysis and kinetic studies of coconut copra and rice husk for possible maximum production of pyrolysis oil", Journal of Cleaner Production, 2017 Crossref	9 words — < 1%
13	hdl.handle.net Internet	8 words — < 1%
14	Aysu, Tevfik, and Halil Durak. "Pyrolysis of giant mullein (<i>Verbascum thapsus</i> L.) in a fixed-bed reactor: Effects of pyrolysis parameters on product yields and character", Energy Sources Part A Recovery Utilization and Environmental Effects, 2016. Crossref	8 words — < 1%
15	www.hindawi.com Internet	8 words — < 1%
16	www.mdpi.com Internet	8 words — < 1%
17	eprints.nottingham.ac.uk Internet	8 words — < 1%

18 Lappas, C. Athanassiou. "Investigating the potential for energy, fuel, materials and chemicals production from corn residues (cobs and stalks) by non-catalytic and catalytic pyrolysis in two reactor configurations", Renewable and Sustainable Energy Reviews, 2009 7 words — < 1%
Crossref

19 Developments in Thermochemical Biomass Conversion, 1997. 7 words — < 1%
Crossref

20 Adrian Chun Minh Loy, Darren Kin Wai Gan, Suzana Yusup, Bridgid Lai Fui Chin et al. "Thermogravimetric kinetic modelling of in-situ catalytic pyrolytic conversion of rice husk to bioenergy using rice hull ash catalyst", Bioresource Technology, 2018 7 words — < 1%
Crossref

21 Saori Ashida, Noboru Katayama, Kiyoshi Dowaki, Mitsuo Kameyama. "A Study on Transient Behavior of Off-gas Impurity Concentration from Metal Hydride", 2018 7th International Conference on Renewable Energy Research and Applications (ICRERA), 2018 6 words — < 1%
Crossref

22 Adrian Chun Minh Loy, Suzana Yusup, Man Kee Lam, Bridgid Lai Fui Chin, Muhammad Shahbaz, Ayaka Yamamoto, Menandro N. Acda. "The effect of industrial waste coal bottom ash as catalyst in catalytic pyrolysis of rice husk for syngas production", Energy Conversion and Management, 2018 6 words — < 1%
Crossref